Carbon Ad-Dimer Defects in Carbon Nanotubes

M. Sternberg,[1] L. A. Curtiss,[1] D. M. Gruen,[1] G. Kedziora,[2,1] D. A. Horner,[3,1] P. C. Redfern,[1] and P. Zapol[1,*]

[1]*Materials Science and Chemistry Divisions, Argonne National Laboratory, Argonne, Illinois 60439, USA*
[2]*High Performance Technologies, Inc., 2435 5th Street, Wright Patterson Air Force Base, Ohio 45433, USA*
[3]*North Central College, 30 North Brainard Street, Naperville, Illinois 60540, USA*

(Received 30 November 2005; published 23 February 2006)

The adsorption of carbon dimers on carbon nanotubes leads to a rich spectrum of structures and electronic structure modifications. Barriers for the formation of carbon dimer induced defects are calculated and found to be considerably lower than those for the Stone-Wales defect. The electronic states introduced by the ad-dimers depend on defect structure and tube type and size. Multiple carbon ad-dimers provide a route to structural engineering of patterned tubes that may be of interest for nanoelectronics.

DOI: 10.1103/PhysRevLett.96.075506 PACS numbers: 81.07.De, 61.46.−w, 73.22.−f, 73.63.Fg

Carbon nanotubes (CNTs) have held promise for use in molecular electronic devices [1,2] since the demonstration of a nanotube as a working transistor [3]. More recently, progress toward using CNTs in quantum computing has been made by using a CNT with defects in conjunction with tunable gates [4]. Defects in the tube wall change the electronic properties of CNTs and can lead to interesting new applications. One example is the role defects play in creating quantum dots with CNTs [5]. Quantum dot behavior was first experimentally observed in single-wall nanotubes [6] and later modeled by using combinations of 5-7 defects (pentagon-heptagon pair) to connect tubes of different helicity and size [7]. Chico *et al.* proposed tube-tube junctions formed by 5-7 defects [8] that were later observed using scanning-tunneling microscopy (STM) and spectroscopy (STS) [9]. A direct comparison of STS plots to theoretical local densities of states (LDOS) illuminates the changes in electronic structure of CNTs due to defects and junctions [10,11]. Stone-Wales (SW, 5-7-7-5) and other combinations of 5-7 defects have been the focus of much work on CNTs investigating their effects on the band structure and transport properties and, in particular, their role in creating intramolecular junctions.

The theoretical work of Orlikowski *et al.* [12] introduced the 7-5-5-7 defect obtained by the addition of a C_2 dimer to a strained CNT and proposed a mechanism based on it for forming junctions. Later, they characterized the defect with a theoretically produced STM image and STS spectrum [13]. In this Letter we demonstrate that there is a rich range of defect structures and electronic structure modification made possible by the reaction of carbon dimers with a CNT. Most significantly, this computational study reveals that for an *unstrained* tube the barrier for formation of the 7-5-5-7 defect is much lower than that for the 5-7-7-5 defect and that the electronic states introduced by this defect depend on the structure and type of CNT. The properties of the C_2 defects discussed here potentially open the way for structural engineering of CNTs that is of special interest for nanoelectronics.

We have used a density functional based tight binding method (DFTB) [14], which has proven reliable for studies on a variety of carbon based materials. Geometry optimizations were performed on armchair (n, n) and zigzag $(n, 0)$ tube models of various radius and length, subject to periodic boundary conditions. To study the effect of large radii (i.e., weak bending), calculations were also performed on bent finite graphene sheets [15].

Adsorbate structures resulting from the addition of C_2 to the surfaces of CNT were investigated for tubes with radii between 3.0 Å and 90 Å. Two configurations are energetically favored. The first is a ''horizontal'' structure, labeled H, where C_2 inserts into two bonds across the hexagon. These bonds break, resulting in two adjacent pentagons between two heptagons, i.e., the 7-5-5-7 defect. The second structure is a ''vertical'' configuration, labeled V, characterized by a single-ended cyclopropyl linkage to just one hexagon bond. By symmetry, two orientations are possible for each structure in the context of each type of tube. On an armchair tube, the horizontal ad-dimer may be oriented either along the axial or a helical direction, denoted H_{ax} and H_{he}, respectively, and the vertical structure may involve either a circumferential or helical bond, denoted V_{circ} and V_{he}. The adsorbate structures on a (5, 5) armchair tube are illustrated in Fig. 1, along with a SW defect. On an $(n, 0)$ tube, the orientations are turned by 30° about the tube normal and accordingly denoted H_{he}, H_{circ}, V_{he}, and V_{ax}.

The energies of the adsorption structures as a function of CNT radius and type are shown in Fig. 2. The H structure shows the strongest dependence on both parameters. Electronic rehybridizations due to the pentagonal rings result in a locally distorted structure that is best accommodated on a small-radius tube with the dimer oriented axially, making the H_{ax} configuration the most stable. For the smallest tube investigated [$r = 3.4$ Å for a (5, 5) tube] the reaction energy is -6 eV. Changing either parameter, i.e., orienting the dimer off axis towards H_{circ}, or increasing the radius, introduces significant stress, evidenced by a rise

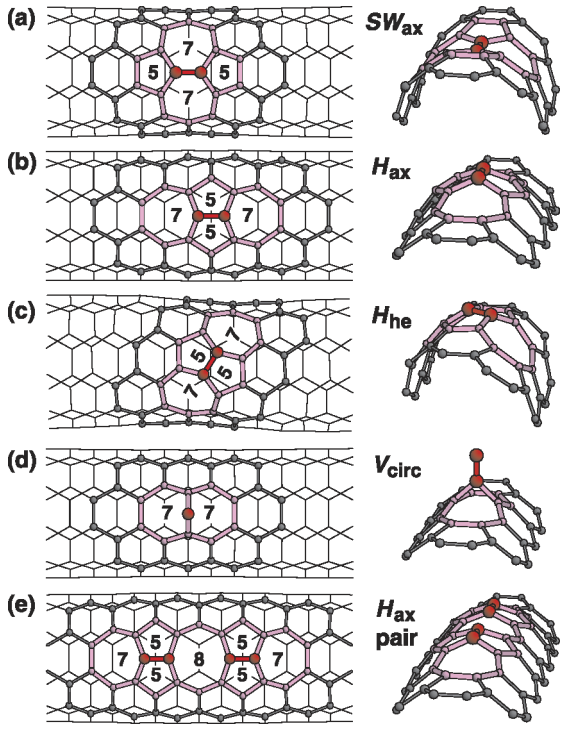

FIG. 1 (color online). Bonding structure of carbon dimer defects on a sample armchair (5, 5) nanotube. (a) Stone-Wales defect, the result of a bond rotation, (b)–(e) ad-dimer defects. The central carbon dimers are shown in red (black). Defected rings are labeled, with bonds shown in magenta (light gray), and surrounding hexagons are shown with dark gray bonds.

in energy over 4–5 eV in either case. By contrast, the V structure is accommodated with little strain and therefore, its energy varies less, from −3.5 eV to −1.9 eV. Since the orientational distinctions with respect to the tube axis vanish for increasing radii, all energies converge with increasing tube radius to separate but very close values for H and V on flat graphene (−1.7 eV and −1.9 eV, respectively).

Interestingly, the addition of a second carbon dimer to a hexagon adjacent to and in line with an existing H_{ax} structure results in an H_{ax} pair structure with an octagon

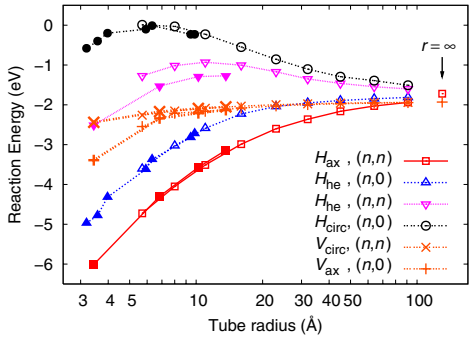

FIG. 2 (color online). Adsorption energy for C_2 defects as function of tube radius and tube type. Closed symbols indicate results from nanotube supercell models, and open symbols represent results from hydrogen-saturated curved graphene sheets.

in the center, as shown in Fig. 1(e). It is energetically more favorable by 0.4 eV to insert two C_2's in this manner than two separated H_{ax} structures. We note that there are numerous other possible arrangements for the addition of successive dimers.

An investigation of the potential energy surface revealed that there is no barrier for the insertion of the end of a C_2 dimer into the CNT wall that results in a metastable V structure. The subsequent ad-dimer tilt to form an H structure (the 7-5-5-7 defect) does have a barrier that depends on tube size. These barriers are listed for selected radii in Table I for H_{ax} on armchair tubes and H_{he} on zigzag tubes, i.e., the most stable structures. The barriers for these orientations increase with increasing tube radius and vary from 1.8 eV to 3.6 eV. We conclude that small tubes are most favorable for the formation of 7-5-5-7 defects, with a reaction energy of −5 to −6 eV and barriers of around 2.5 eV.

There is quite possibly an experimental confirmation for the suggested existence of two steps in the addition of C_2. It is known that irradiation of a graphite substrate with high-energy argon ions can result in C_2 production. Osváth *et al.* [16] examined nanotubes supported on graphite that were irradiated by 30 keV Ar^+ ions. The STM investigation found hillocklike protrusions of 2.42 Å before annealing and 0.92 Å after annealing at 450 °C, close to our calculated heights of the vertical (2.72 Å) and horizontal axial (0.95 Å) ad-dimer configurations, respectively.

For the purpose of an energy comparison with the SW defect [cf. Fig. 1(a)], a C_2 ad-dimer can be viewed as a di-interstitial intrinsic defect in the CNT. The formation energy of H_{ax} with respect to the nanotube is smaller by as much as 1 eV than that of a SW defect for CNT radii below 7 Å, making the 7-5-5-7 (H) defect thermodynamically more favorable than the 5-7-7-5 (SW) defect for most CNT sizes. In addition, the calculated barrier for formation of the 7-5-5-7 defect can be as small as 1.8 eV, much smaller than for the SW defect, where it is above 6 eV for strain below 5% [17]. Thus, it seems that the 7-5-5-7 defect is potentially a more attractive way for introducing defects into a CNT in a controlled way than the SW defect.

To explore the possible variation of the electronic properties of the nanotubes we calculated the local densities of states (LDOS) of the various defects; cf. Fig. 3. Different peaks are clearly associated with different defect struc-

TABLE I. Energy barriers for the conversion of V to H structures on armchair and zigzag CNTs, obtained from bent graphene sheet models.

Radius (Å)	Barrier (eV)	
	$V_{circ} \rightarrow H_{ax}$	$V_{he} \rightarrow H_{he}$
3.3	2.3	1.8
5.7	2.4	2.6
11.0	2.9	3.2
∞	3.6	3.6

tures. The helical SW defect does not introduce new electronic states (and was therefore omitted from the plot), whereas the axial SW defect produces a level in the conduction band at about $E_F + 0.7$ eV. Interestingly, the vertical C_2 defect has a level located at about the same energy. Therefore, it would be difficult to distinguish peaks associated with these two defects in STS spectra. However, the horizontal C_2 defect (H_{ax}) provides a clear and unambiguous peak at $E_F - 0.5$ eV, which might be observed experimentally and serve as a means to monitor the defect concentration by its intensity. The double dimer defect, H_{ax} pair, has a split peak centered around $E_F - 0.5$ eV. We found little dependence of the location of any H peak on tube radius, with the exception of a somewhat noticeable difference between semimetallic and semiconducting zigzag $(n, 0)$ tubes, illustrated in Fig. 3 for the cases $n = 9$ and $n = 10$.

In several STS studies [9,11,18] measurements of $dI/dV(V/I)$ were compared to theoretical densities of states. Some of these data for a number of tubes show a small peak near $E_F - 0.5$ eV, which is not discussed. A comparison of local STS results [18] from the middle and near the end of the tubes excludes caps as the origin of this peak. We suggest that the peak may be due to the H defect. Notice also that calculated densities of states for perfect tubes [9,11,18] do not show peaks in this energy region.

The C_2 defects found in this study are an attractive route for modification of carbon nanotubes due to their stabilities and the fact that the vertical adsorbate has no barrier to insertion and the horizontal one has a significant barrier. The reaction of C_2 with carbon nanotubes has remarkable similarities to the role of C_2 in the growth of chemical vapor deposition diamond where it was demonstrated that C_2 produced by fragmentation of fullerene molecules in a microwave discharge leads to the growth of ultrananocrystalline diamond (UNCD) films [19]. Extensive electronic structure calculations have shown that C_2 inserts into various faces of diamond without a barrier and can result in both growth of diamond and nucleation of new diamond crystallites [20,21]. Analogous to UNCD, the vertical adsorbate on CNTs can act as a nucleation site of a new nanocarbon phase on the CNT, which can be controlled by the kinetics and thermodynamics of C_2 addition. Alternatively, if kinetics favors horizontal addition, expansion of the CNT might occur as shown in Fig. 4(a).

If addition of the C_2 is done with both kinetic and spatial control a number of interesting modifications to the CNT structure are possible. The "bumpy" tube in Fig. 4(b) has C_2 dimers added symmetrically around the circumference of a $(5, 5)$ tube to create a stable bulge. The control of spacing between the bulges could be used to make well-defined quantum dots. The "zipper" tube shown in Fig. 4(c) has C_2 dimers added in horizontal orientation along the axial direction of a (n, n) tube to every other hexagon resulting in alternating single octagons and pairs of pentagons, i.e., an extended H_{ax} pair structure. As can be seen from Fig. 5 the DOS for this tube indicates that it remains metallic and has new electronic states introduced near the Fermi level. The spacing on the zipper structure is a very good match for the diamond (100) surface for possible formation of diamond—CNT composites. The "multiple zipper" tube in Fig. 4(d) has six axial "zippers" spaced by hexagon rows around a $(6, 6)$ tube. The total DOS for these tubes given in Fig. 5 shows metallic character with additional peaks introduced near the Fermi level. This resembles the previously proposed Haeckelite tubes [22,23] that are composed of heptagons and pentagons, and

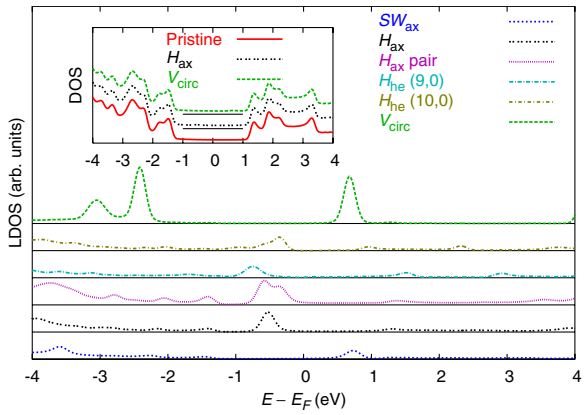

FIG. 3 (color online). Electronic local density of states (LDOS) for defects on single-wall carbon nanotubes. The inset shows the total DOS for selected structures, indicating no significant changes due to isolated adsorbates.

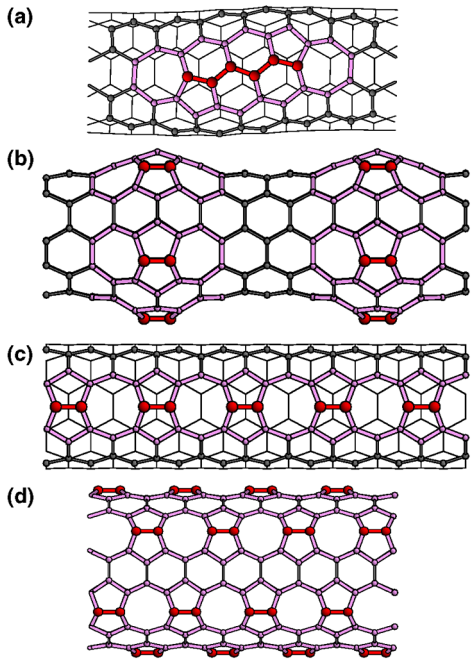

FIG. 4 (color online). Structure of multiple C_2 adsorbates: (a) local expansion of a $(5, 5)$ CNT, (b) alternating adsorbates around the circumference of a $(5, 5)$ tube, (c) a $(5, 5)$ CNT with alternating adsorbates in an axial direction resulting in a zipper tube, and (d) a $(6, 6)$ CNT with multiple staggered "zippers."

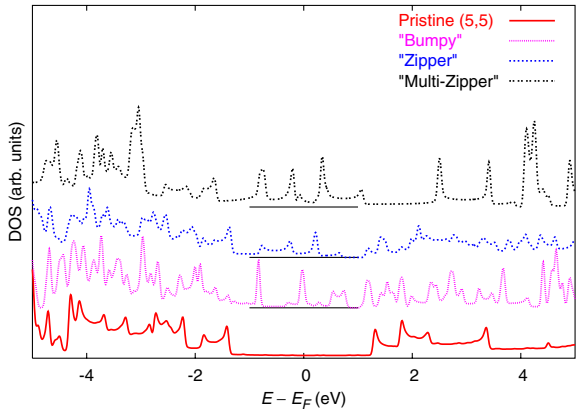

FIG. 5 (color online). Electronic DOS for structures shown in Figs. 4(b)–4(d) and comparison with a pristine (5, 5) tube.

are proposed to have superconducting properties. We note that a Haeckelite structure could in fact be created by appropriate addition of carbon dimers to an armchair tube.

In conclusion, two new features predicted by this study make the family of C_2 defects very attractive. First, the barrier for formation of the 7-5-5-7 defect is much lower than that of the SW defect, which means that C_2 insertion is therefore likely to be realized in practice using well-established experimental techniques, such as those for the growth of UNCD from this species [19]. Second, the electronic states introduced by the defects depend on the defect structure and type of the CNT. Peaks arising in the DOS in close proximity of the Fermi level due to reactions with C_2 tend to be associated with localized electrons. Defect formation in CNTs appears to open up a wide window for the manipulation of such electronic states, especially when multiple C_2 defects are added to the CNTs. It has been theoretically predicted and experimentally shown that low dimensional materials frequently possess DOS characteristics similar to those observed in the defected nanotubes that are the subject of this Letter. Such nanomaterials often display substantially improved thermoelectric performance [24,25]. Therefore, success in controlling the introduction of defects would provide one with an unparalleled opportunity for creating entirely new device functionalities.

This work was supported by the Division of Materials Science, Office of Basic Energy Sciences, U.S. Department of Energy, under Contract No. W-31-109-ENG-38.

*Electronic address: zapol@anl.gov

[1] P. L. McEuen, Nature (London) **393**, 15 (1998).
[2] C. Dekker, Phys. Today **52**, No. 5, 22 (1999).
[3] S. J. Tans, A. R. M. Verschueren, and C. Dekker, Nature (London) **393**, 49 (1998).
[4] N. Mason, M. J. Biercuk, and C. M. Marcus, Science **303**, 655 (2004).
[5] M. J. Biercuk, N. Mason, J. M. Chow, and C. M. Marcus, Nano Lett. **4**, 2499 (2004).
[6] S. J. Tans, M. H. Devoret, H. Dai, A. Thess, R. E. Smalley, L. J. Georliga, and C. Dekker, Nature (London) **386**, 474 (1997).
[7] L. Chico, M. P. López Sancho, and M. C. Muñoz, Phys. Rev. Lett. **81**, 1278 (1998).
[8] L. Chico, V. H. Crespi, L. X. Benedict, S. G. Louie, and M. L. Cohen, Phys. Rev. Lett. **76**, 971 (1996).
[9] M. Ouyang, J.-L. Huang, C. L. Cheung, and C. M. Lieber, Science **292**, 702 (2001).
[10] V. Meunier and P. Lambin, Phil. Trans. R. Soc. A **362**, 2187 (2004).
[11] M. Ouyang, J.-L. Huang, and C. M. Lieber, Acc. Chem. Res. **35**, 1018 (2002).
[12] D. Orlikowski, M. B. Nardelli, J. Bernholc, and C. Roland, Phys. Rev. Lett. **83**, 4132 (1999).
[13] D. Orlikowski, M. Buongiorno Nardelli, J. Bernholc, and C. Roland, Phys. Rev. B **61**, 14 194 (2000).
[14] Th. Frauenheim, G. Seifert, M. Elstner, T. Niehaus, C. Köhler, M. Amkreutz, M. Sternberg, Z. Hajnal, A. Di Carlo, and S. Suhai, J. Phys. Condens. Matter **14**, 3015 (2002).
[15] For (n, n) tubes we selected: $n \in \{5, 10, 15, 20\}$, and for $(n, 0)$: $n \in \{8, 9, 10, 15, 16, 24, 25\}$. Supercells containing tube segments approximately 25 Å long were used for geometry optimization. One ring of atoms was kept frozen to reduce periodic image interaction. The $\boldsymbol{k}$ space was sampled at the Γ point. For density-of-state calculations of isolated defects supercells were extended to approximately 200 Å. The graphene sheets measure approximately 30 Å laterally and were hydrogen terminated and frozen along the zigzag edges.
[16] Z. Osváth, G. Vértesy, L. Tapasztó, F. Wéber, Z. E. Horváth, J. Gyulai, and L. P. Biró, Phys. Rev. B **72**, 045429 (2005).
[17] Q. Zhao, M. B. Nardelli, and J. Bernholc, Phys. Rev. B **65**, 144105 (2002).
[18] P. Kim, T. W. Odom, J.-L. Huang, and C. M. Lieber, Phys. Rev. Lett. **82**, 1225 (1999).
[19] D. M. Gruen, Annu. Rev. Mater. Sci. **29**, 211 (1999).
[20] M. Sternberg, P. Zapol, and L. A. Curtiss, Phys. Rev. B **68**, 205330 (2003).
[21] D. M. Gruen, P. C. Redfern, D. A. Horner, P. Zapol, and L. A. Curtiss, J. Phys. Chem. B **103**, 5459 (1999).
[22] H. Terrones, M. Terrones, E. Hernandez, N. Grobert, J.-C. Charlier, and P. M. Ajayan, Phys. Rev. Lett. **84**, 1716 (2000).
[23] J.-C. Charlier, Acc. Chem. Res. **35**, 1063 (2002).
[24] Y.-M. Lin and M. S. Dresselhaus, Phys. Rev. B **68**, 075304 (2003).
[25] K. Bradley, S.-H. Jhi, P. G. Collins, J. Hone, M. L. Cohen, S. G. Louie, and A. Zettl, Phys. Rev. Lett. **85**, 4361 (2000).